Cell, Vol. 87, 543–552, November 1, 1996, Copyright ©1996 by Cell Press

Familial Hemiplegic Migraine and Episodic Ataxia Type-2 Are Caused by Mutations in the Ca^{2+} Channel Gene CACNL1A4

Roel A. Ophoff,[1,2] Gisela M. Terwindt,[2] Monique N. Vergouwe,[1,2] Ronald van Eijk,[1,2] Peter J. Oefner,[3] Susan M. G. Hoffman,[4,8] Jane E. Lamerdin,[4] Harvey W. Mohrenweiser,[4] Dennis E. Bulman,[5] Maurizio Ferrari,[6] Joost Haan,[2] Dick Lindhout,[7] Gert-Jan B. van Ommen,[1] Marten H. Hofker,[1] Michel D. Ferrari,[2] and Rune R. Frants[1]

[1]MGC—Department of Human Genetics
Sylvius Laboratory
Leiden University
Wassenaarseweg 72
2333 AL Leiden
[2]Department of Neurology
Leiden University Hospital
Albinusdreef 2
2333 ZA Leiden
The Netherlands
[3]Department of Genetics
Stanford University
Stanford, California 94305
[4]Lawrence Livermore National Laboratory
BBRP
Livermore, California 94550
[5]Department of Clinical Neurological Sciences
London Health Sciences Centre
London, Ontario N6A 5A5
Canada
[6]Clinical Molecular Biology Laboratory
IRCCS S. Raffaele
Via Olgettina 60
20132 Milan
Italy
[7]MGC—Department of Clinical Genetics
Erasmus University Rotterdam
3000 DR Rotterdam
The Netherlands

Summary

Genes for familial hemiplegic migraine (FHM) and episodic ataxia type-2 (EA-2) have been mapped to chromosome 19p13. We characterized a brain-specific P/Q-type Ca^{2+} channel α1-subunit gene, CACNL1A4, covering 300 kb with 47 exons. Sequencing of all exons and their surroundings revealed polymorphic variations, including a $(CA)_n$-repeat (D19S1150), a $(CAG)_n$-repeat in the 3′-UTR, and different types of deleterious mutations in FHM and EA-2. In FHM, we found four different missense mutations in conserved functional domains. One mutation has occurred on two different haplotypes in unrelated FHM families. In EA-2, we found two mutations disrupting the reading frame. Thus, FHM and EA-2 can be considered as allelic channelopathies. A similar etiology may be involved in common types of migraine.

[8]Present address: Department of Zoology, Miami University, Oxford, Ohio.

Introduction

Migraine is a frequent, neurological disorder, characterized by recurrent attacks of disabling headache, vomiting, photo- and phonophobia, and malaise (migraine without aura). In 20% of patients, additional transient focal neurological (aura) symptoms may occur (migraine with aura) (Headache Classification Committee, 1988). Up to 24% of females and 12% of males in the general population are affected by migraine, although frequency, duration, and severity of the attacks vary substantially across patients (Russell et al., 1995).

Family, twin, and population-based studies suggest that genetic factors are involved in migraine, most likely as part of a multifactorial mechanism (Russell and Olesen, 1995; Haan et al., 1996). The complex genetics has, thus far, hampered identification of candidate genes. Familial hemiplegic migraine (FHM), a rare autosomal dominant subtype of migraine with aura, is associated with ictal hemiparesis and, in some families, progressive cerebellar atrophy (Headache Classification Committee, 1988; Terwindt et al., 1996). Otherwise, the symptoms of the headache and aura phase of FHM and "normal" migraine attacks are very similar, and both types of attack may alternate within individuals and cooccur within families. FHM is thus part of the migraine spectrum and can be used as a model to study the complex genetics of the more common forms of migraine.

A gene for FHM has been assigned to chromosome 19p13 in about 50% of the families tested (Joutel et al., 1993; Ophoff et al., 1994, 1996; Joutel et al., 1994). Cerebellar atrophy was found only in FHM families linked to chromosome 19p13 (Terwindt et al., 1996). Recently, the region containing the 19p13 FHM locus was shown to be also involved in the more common forms of migraine (May et al., 1995), adding to the hypothesis that FHM is part of the migraine spectrum involving similar genetic factors and biological mechanisms.

Episodic ataxia type 2 (EA-2) is another autosomal dominant paroxysmal cerebral disorder, characterized by acetazolamide-responsive attacks of cerebellar ataxia and migraine-like symptoms, interictal nystagmus, and cerebellar atrophy (Von Brederlow et al., 1995). Recently, a locus for EA-2 was mapped to chromosome 19p13, in the same interval as the FHM locus (Kramer et al., 1995; Von Brederlow et al., 1995; Teh et al., 1995). This finding, in addition to the clinical similarities, raises the possibility that EA-2 and FHM are allelic disorders.

Since other hereditary acetazolamide-responsive episodic neurological disorders, such as hypokalemic and hyperkalemic periodic paralysis, as well as EA type-1, have all been associated with mutations in ion channel genes (Ptacek et al., 1991, 1994; Browne et al., 1994; Jurkatt-Rott et al., 1994; Griggs and Nutt, 1995), we specifically searched for similar genes within the FHM and EA-2 candidate region.

Using exon trapping, we identified a human cDNA, highly related to a brain-specific rabbit and rat voltage gated P/Q-type Ca^{2+} channel α1 subunit (Mori et al.,

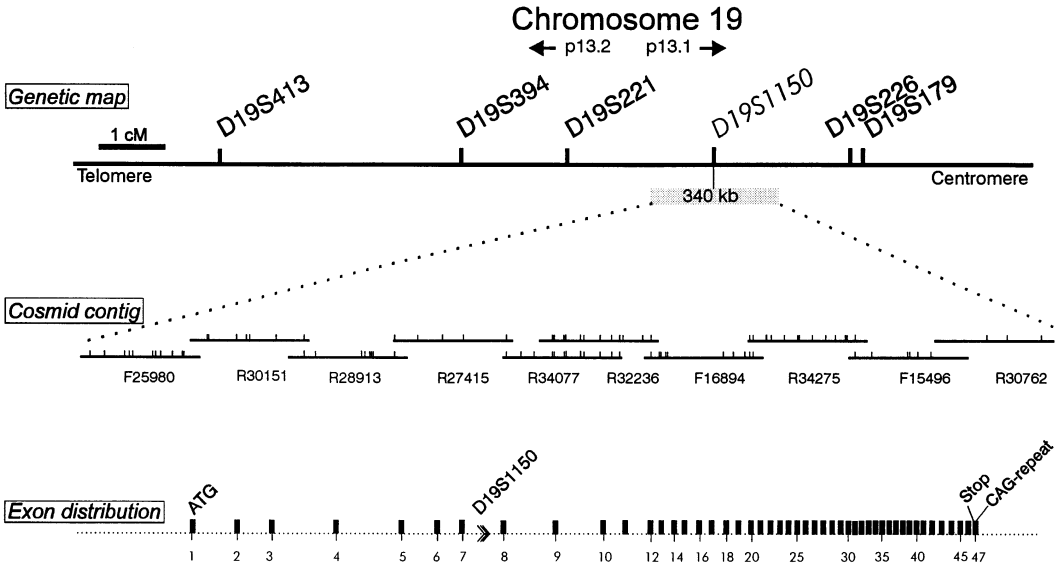

Figure 1. Genetic Map, Cosmid Contig, and Global Exon Distribution of the CACNL1A4 Gene on Chromosome 19p13.1

Cosmid contig is shown with EcoRI restriction sites, available via Lawrence Livermore National Laboratory (LLNL); exon positions are indicated schematically, regardless of exon or intron sizes (Table 1). D19S1150 is a highly polymorphic intragenic $(CA)_n$-repeat.

1991; Starr et al., 1991). The human gene was designated CACNL1A4 (Diriong et al., 1995). The gene contains an open reading frame that encodes a protein of 2261 amino acids. Because of the brain-specific expression, and its putative ion channel function, CACNL1A4 was considered an excellent candidate gene for FHM and EA-2. The genomic structure was elucidated and mutation analysis was performed, applying single strand conformational polymorphism (SSCP) and denaturing high-performance liquid chromatography (DHPLC). The results indicate that missense mutations in the α1 subunit cause FHM, while truncating mutations in the same protein cause EA-2. These findings imply that FHM, EA-2, and possibly also the more common types of migraine are ion channel disorders and provide yet another example in the growing list of ion channel disorders in which remarkable phenotypic heterogeneity is associated with different types and positions of mutations.

Results

cDNA Sequence

Eight cosmids, forming two small contigs in the FHM candidate region between markers D19S394 and D19S226 (Figure 1), were subjected to exon trapping. Five different clones were identified, showing a highly similar (≥90%) sequence to rabbit (EMBL X57476) and rat (Genbank M64373) cDNA, both encoding a brain-specific P/Q-type Ca^{2+} channel α1 subunit (Mori et al., 1991; Starr et al., 1991). These clones most likely represented five adjacent exons of the human ortholog of the Ca^{2+} channel gene from position 292 to 985 (positions based on rat cDNA sequence). A BLAST search using the 3′-end of the rat cDNA (position 6000–6638) revealed a human EST (GenBank U06702), again with very high similarity (92%) (Margolis et al., 1995). The different fragments of the cDNA sequences were amplified from total human cerebellum cDNA (Clontech) by PCR and were used as probes for screening the same cerebellum library (Clontech). Assembly of the complete coding sequence of the human cDNA showed an open reading frame of 6783 nucleotides, which encodes for a putative protein of 2261 amino acids (EMBL X99897). Recently, a neuronal Ca^{2+} α1A-subunit gene was localized to chromosome 19p13.1-p13.2 by FISH analysis (Diriong et al., 1995). The gene symbol is CACNL1A4 and the α1 subunit is classified as a P/Q-type. Although no sequence data for the CACNL1A4 gene are available yet, the same localization (chromosome 19p13.1) and the identical classification (P/Q-type) strongly suggest that the Ca^{2+} channel α1 subunit we have identified is CACNL1A4.

Genomic Structure

The cosmid contig that yielded the initial Ca^{2+} channel gene exons was extended to cover more than 300 kb and has been placed into the Lawrence Livermore National Laboratory (LLNL) physical map of chromosome 19 at band p13.1 (Figure 1). Initial hybridization experiments showed that the first and the last cosmids of this contig were positive for 3′- and 5′-end cDNA sequences, respectively. Therefore, all 10 cosmids of the contig (Figure 1) were randomly subcloned. Subsequently, clones containing exons were selected by hybridization using overlapping CACNL1A4 cDNA probes (EMBL X99897) and sequenced using vector- and exon-specific primers. Complete alignment between the cDNA and individual exon sequence was achieved, allowing establishment of the exon–intron structure (Table 1). The CACNL1A4 gene is composed 47 exons ranging in size from 36 bp (exon 44) to 810 bp (exon 19). Exon 1 includes the start codon and the untranslated 5′ region. The stop codon,

Table 1. Exon/Intron Organization of the Human CACNL1A4 Gene and Exon-Specific Primer Pairs

Exon	cDNA	Size	Domain	Cosmid(s)	Primer Forward	Primer Reversed	Size
1	UTR–568	≥500		25960/30151	tct ccg cag tcg tag ctc ca	ggt tgt aga gtg cca tgg tc	320
					cgc aaa gga tgt aca agc ag	att ccc aag cct cca ggg tag	370
2	569–674	106	I S1	30151	cac ctc caa cac cct tct tt	tct gtg ccc tgc tcc act c	240
3	675–814	140	I S2, I S3	30151	acg ctg acc ttg cct tct ct	caa cca aaa gcc tcg taa tc	230
4	815–906	92	I S3, I S4	28913	aaa acc cac cct ctg ttc tc	ttg tca ggg tcg gaa act ca	160
5	907–1059	153	I S5	28913/27415	ctt ggt ggc ggg gtt t	ctg cct aat cct ccc aag ag	290
6	1060–1253	194		27415	tcc ctt ccc ttt tgt aga tg	gtg ggg ctg tgt tgt cct t	350
7	1254–1357	104	I S6	27415	gac aga gcc aca aga gaa cc	agc aaa gag gag tga gtg gg	250
8	1358–1473	116		34077/27415	ata ctc tgg ctt ttc tat gc	gca tga ctc tct ttg tac tc	230
9	1474–1530	57		34077	gca gag aat ggg ggt gg	ctg agg tgg gtt tag agc ag	180
10	1531–1623	93		34077	ggg taa cgt ctt ttt ctc ttg c	atg tct ctt ggg cga tag gt	200
11	1624–1833	210	II S1	16894/32236	att tct tct gaa gga aca gc	gga ggg atc agg gag ttg gc	310
12	1834–1946	113	II S2, II S3	16894	caa gcc taa cct cct ctc tg	tca ttc cag gca aga gct g	200
13	1947–2051	105	II S3, II S4	16894	att tgg agg gag gag ttt gg	tca ctt tcc caa ctt tct gg	310
14	2052–2191	140	II S4, II S5	16894	cag aaa gtt ggg aaa gta gc	ttg aat tcc tgt gaa gga c	250
15	2192–2264	73		16894	ctt gga gat gag ata ctg agc	cag gca ctt tca tct gtg ac	200
16	2265–2382	118	II S6	16894	tcc aca gct gca tct cca ag	acc ctc cct tga gcc cct	270
17	2383–2450	68	II S6	16894	cag tgg ttg ctt ttc ctg ac	ttg cca gag aaa cat tct cc	130
18	2451–2557	107		16894	tga aca aag att cca cgt gc	ttc agg agc cag ggt agc atc	170
19	2558–3367	810		16894	tag caa tgc tct aag tcc tg	tgt ttc ctg agg aag tcc tc	320
					cgc agg aga acc gca aca a	gcg atg acg tcg atg ctc	450
					gc agc agg gag agc cgc agc	tac cgt cat tct gcg gat tc	300
20	3368–3831	464		16894	ggt tct ttt tca ttc act tgc	ttt cct ggc agt ctt agc tg	430
					gag aat agc ctt atc gtc ac	cag tga tgt gag agc aga g	200
21	3832–3973	142		16894/34275	tgg gaa att gtg gag gga gc	tga ctt ccg cca ccc tgg tg	250
22	3974–4103	130	III S1	16894/34275	agc ctg tgg tct gag tgg ac	tag gaa ggg gtg tgc tct gtg	210
23	4104–4163	60	III S2, III S3	16894/34275	atc cac tgc tct ctt gct tt	gtg gtt ctc act tat aat ctg c	170
24	4164–4270	107	III S3	34275	tgg cct cat tgg ctt ccc tgc	aag agg aaa ccc ttg cga ag	250
25	4271–4370	100	III S4	34275	cta ccc aac ctg acc tct gc	aca tga taa ccc tga cag tc	220
26	4371–4531	161	III S5	34275	ctc atg ctc tct gtc aac tc	tgg ttc caa tgg gaa tgt gc	250
27	4532–4669	138		34275	ctg ctt ccc aag cag tct ag	tcc tgg ata gat ttc cag tc	300
28	4670–4871	202	III S6	34275	agt ttt taa agg aca gat gg	ttt ccc tgc ccc att cct ttg c	280
29	4872–5036	165	IV S1	34275	ctc tgc cgc tct cac cac tg	ttt atc agg tag agg cag g	250
30	5037–5147	111	IV S1, IV S2	34275	ttc caa gcc cat agc tgt agc	tga ccc tgc tac tcc tgc ttc	180
31	5148–5231	84	IV S3	15496	act gtg cct cta aca tgc ac	aag tgc tgg ctc aag cag	250
32	5232–5348	117	IV S4	15496	tct gtg agt ggt gac agc tc	gtc acc tgt ctt ctc agc	240
33	5349–5414	66	IV S5	15496	tgg aag gac tct ggc acg tg	gga ggc tct ggg aac ctt ag	250
34	5415–5530	116		15496	aga agc cac tgg agg aat ggc	att atc aga gca ggt ccc ctt c	250
35	5531–5681	151	IV S6	15496	tcc gag tct ctg att tct cc	aga cgg ccc tca cag tgt c	210
36	5682–5809	128	IV S6	15496	ttc att ccc tcg gtc tct gc	ctg act gaa cct gtg aga c	350
37	5810–5906	97		15496	tgt gaa ccc att gcc tgc a	tgg gaa tga ctg cgc ttg c	200
38	5907–6012	106		15496	atg cct ggg aat gac tgc	tgt cac gcc tgt ctg tgc	200
39	6013–6120	108		15496	tga cac cca ggc agg cag	tct gtc ctg gtg gat tgg atc	200
40	6121–6221	101		15496	ttg gtg agc tca ccg tgt	ttc ccg tgg tga cat gca agc	200
41	6222–6331	110		15496	gtc cac aca ctg ctc tct gc	aca ctc cac ctc cct ggc	320
42	6332–6470	139		15496	gcc agg gag gtg gag tgt	ggt tcc ttc cac cgc aac	550
43	6471–6584	114		15496/30762	caa ctc ccc aat ggc tc	cct acc cag tgc aga gtg agg	350
44	6585–6620	36		15496/30762	tct gtg tgc acc atc cca tg	aag gat tgg gct cca tgg ag	200
45	6621–6807	187		15496/30762	gtt ggt gct agc tgc tga c	ctt tct tct tcc tta gtg tc	330
46	6808–7061	254		15496/30762	gtg tgc tgt ctg acc ctc ac	agc ctg ggg tca ctt gca gc	320
47	7062–UTR	≥350		30762	cct ttg ttt caa ttt tcg tgt ag	tgg ggc ctg ggt acc tcc ga	280

Sizes of exons and PCR products are given in basepairs; cDNA and genomic sequences are available via EMBL accession no. X99897, Z80114–Z80115, respectively; domains of protein are indicated according to Stea et al., 1995.

as well as the 3′-terminal noncoding region, is located in exon 47. The exons are distributed over ~300 kb DNA. The first 10 exons span ~150 kb and are covered by the first 5 cosmids of the contig (Table 1; Figure 1), which indicates relatively large introns at the 5′ side of the gene. Sequence data was obtained for every exon and ~100 bp of flanking introns, except for the 5′ end of exon 6. Therefore, the forward primer of exon 6 contains the splice junction and 3 bp of exon 6. Splice sites flanking all exons are compatible with consensus sequence with the exception of the splice donor and acceptor of the first intron. Sequence of intron 7 showed a (CA)-repeat sequence, which turned out to be highly polymorphic (D19S1150). Analysis of this dinucleotide repeat revealed nine alleles with an observed heterozygosity of 0.82, in 45 random individuals from the Dutch population. Sequences of all exons and flanking introns are available via EMBL accession numbers Z80114–Z80115.

Northern Blot Analysis

In an initial Northern blot analysis, the spatial distribution of the human CACNL1A4 expression was assayed in rhesus monkey tissues. Total RNA was isolated from

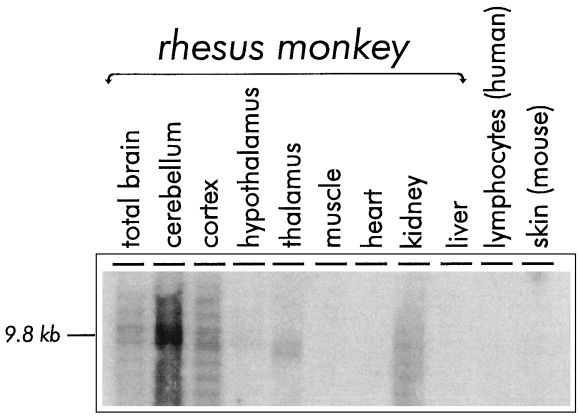

Figure 2. Expression of Human P/Q-Type Calcium Channel α1-Subunit Gene (CACNL1A4) Tested in Different Tissues

Northern blot of total RNA from rhesus monkey tissues (total brain, cerebellum, cortex, hypothalamus, muscle, heart, kidney, liver), human lymphocytes, and mouse skin, hybridized with human cDNA probe 1 (See cDNA Sequence section of Experimental Procedures). Size of transcript was estimated at 9.8 kb.

several tissues, including various brain structures, and probed with a human cDNA fragment (Figure 2). The probe detected a major transcript of approximately 9.8 kb in cerebellum, cerebral cortex, thalamus and hypothalamus, whereas no transcript was detected in heart, kidney, liver, or muscle. There was also no hybridization signal found in RNA preparations from mouse skin tissue or from human peripheral lymphocytes.

Primary Structure of CACNL1A4

Calcium channels are multimeric complexes that are composed of one α1, α2, δ, and a β subunit (Campbell et al., 1988). The central α1 subunit is functionally the most important component and acts as a voltage sensor and forms the ion-conducting pore. The other subunits have auxiliary regulatory roles. Topologically, an α1 subunit consists of four internal homologous repeats (I–IV), each containing six putative α-helical membrane spanning segments (S1–S6) and one pore-forming (P) segment between S5-S6 that spans only the outer part of the transmembrane region (Guy and Durell, 1996). The membrane spanning segments (S1–S6) of domains I–IV are most similar between different classes of Ca^{2+} channel α1 subunits (Stea et al., 1995) and enabled us to predict the putative membrane topology of CACNL1A4 as shown in Table 1 and Figure 3.

Mutation Analysis

All 47 exons and flanking intron sequences were screened for the presence of mutations by SSCP and DHPLC analysis in 20 individuals with either FHM or EA-2. Several synonymous nucleotide substitutions and polymorphisms, including a highly polymorphic $(CAG)_n$-repeat in the 3′ untranslated region of exon 47, were identified by their occurrence in unaffected controls and lack of cosegregation with the disease in families (Table 2). Only the polymorphism in exon 11 predicts an amino acid change, an alanine-to-threonine substitution at codon 454 (A454T).

Four different missense mutations were identified in FHM patients of which one mutation was observed in two unrelated FHM-affected individuals (Table 3; Figure 4). The mutations were shown to segregate with the disease in the corresponding families and were not present in 100 control chromosomes. A transition from G to A was identified in family *It-II* at codon 192, resulting in a substitution of arginine for glutamine (R192Q) within the fourth segment of the first membrane spanning domain (IS4). A second missense mutation occurs at codon 666, within the hairpin loop of the second repeat, replacing a threonine residue for methione (T666M) in family *US-P*. Two other mutations were located in the 6th transmembrane spanning segment of repeats II and IV. The IIS6 mutation is a T-to-C transition at codon 714, resulting in a valine-to-alanine substitution (V714A), and was identified in FHM family *UK-B*. The mutation in domain IVS6 was an A-to-C transversion at codon 1811 that resulted in a substitution of isoleucine for leucine (I1811L). This I1811L mutation was found twice, in family *NL-A* and family *US-C*, which are two unrelated FHM families. Moreover, comparison of haplotypes in this region, including intragenic markers, indicated recurrent mutations on two genetically distinguishable chromosomes (data not shown).

In addition to missense mutations in FHM families,

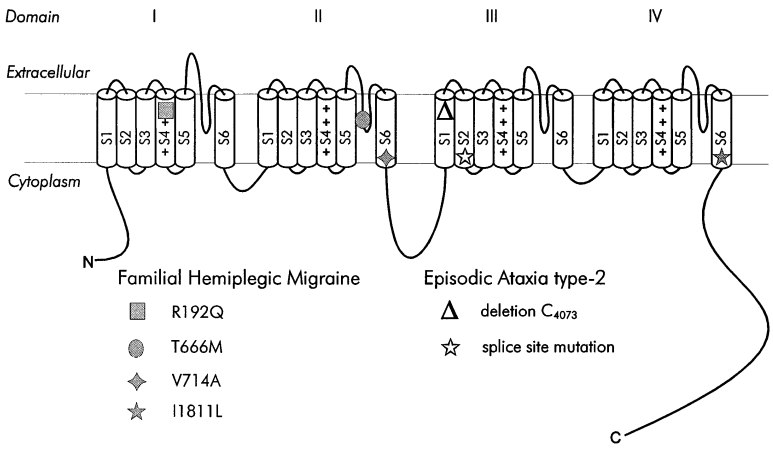

Figure 3. Membrane Topology of α1 Subunit of the P/Q-Type Ca^{2+}-Channel, CACNL1A4

The location and amino acid substitutions are indicated for mutations that cause familial hemiplegic migraine (FHM) and episodic ataxia type-2 (EA-2).

Table 2. Polymorphisms in Coding Sequence of CACNL1A4

Location	Nucleotide Change			Frequency	Consequence
Exon 4	nt 854	G→A	Thr_{193}	0.02	—
Exon 6	nt 1151	A→G	Glu_{292}	0.07	—
Exon 8	nt 1457	G→A	Glu_{394}	0.38	—
Exon 11	nt 1635	G→A	Ala_{454}	0.02	Ala_{454}→Thr (A454T)
Exon 16	nt 2369	G→A	Thr_{698}	0.12	—
Exon 19	nt 3029	G→A	Glu_{918}	0.07	—
Exon 23	nt 4142	T→C	Phe_{1289}	0.22	—
Exon 46	nt 6938	T→C	His_{2221}	0.46	—
Exon 47	nt 7213	$(CAG)_n$	3′UTR	#	—

Frequency as observed in 100 control chromosomes; #, seven alleles of $(CAG)_n$ were observed in the range between n = 4 to n = 14, with a heterozygosity value of 0.75.

we also identified mutations in two out of four EA-2 families (Table 3; Figure 5). In family *CAN-191*, a one nucleotide deletion occurred at position 4073 (codon 1266) causing a frame shift and a premature stop in exon 23, at codon 1333. A second EA-2 mutation was detected in family *CAN-26* in which a transition of G-to-A of the conserved first nucleotide of intron 28 occurred, predicted to cause aberrant splicing. So far, no mutations were found in FHM family *It-I*, in the six sporadic hemiplegic migraine patients, and in two EA-2 families.

Discussion

We have isolated the CACNL1A4 gene, in which we identified mutations in FHM and EA-2 patients, demonstrating these paroxysmal disorders to be allelic. As the CACNL1A4 gene encodes a brain-specific P/Q-type Ca^{2+} channel α1 subunit, FHM and EA-2 can now be considered as cerebral ion channel disorders. Moreover, since FHM is part of the migraine spectrum, further elucidation of this pathway will lead to new insights into the etiology of the more common types of migraine.

Missense Mutations in Familial Hemiplegic Migraine

Four different missense mutations were identified in five unrelated FHM families (Table 3; Figure 4). One of these missense mutations occurred in two unrelated FHM families on different haplotypes, strongly supporting recurrent mutations rather than a founder effect.

In family *It-II*, a mutation was identified in the IS4 domain of CACNL1A4, substituting a positively charged arginine with a neutral, nonpolar glutamine (R192Q). The S4 domains are considered to be the voltage sensors of Ca^{2+} channels and have a conserved, unusual pattern of positively charged arginine residues at every third or fourth position, separated by hydrophobic residues (Tanabe et al., 1987; Stea et al., 1995). The R192Q mutation distorts this conserved higher order structure rendering it plausible that this mutation compromises functioning as a voltage sensor.

The second missense mutation (T666M) was identified in family *US-P* and is located in the pore-forming (P) segment between IIS5 and IIS6 (Figure 3). Various observations have shown that these hairpin structures between each of the S5 and S6 segments in ion channels together form the ion-selectivity filter of the pore and present binding sites for toxins (Guy and Durell, 1996). Alignment of protein sequences of different P segments shows that some residues are conserved in many ion channel genes (Guy and Durell, 1996). The T666M substitution alters one of the conserved residues in the P segment, which makes it likely that the T666M substitution will affect the ion-selectivity or toxin binding ability of the P/Q-type Ca^{2+} channel.

The remaining two missense mutations identified in FHM families alter the S6 segment of the second and the fourth repeat. The mutation in domain IIS6, the V714A substitution, was identified in FHM family *UK-B*, whereas the I1811L mutation, affecting domain IVS6, was present in two unrelated FHM families (*NL-A* and *US-C*). The occurrence of I1811L in two FHM families with a different chromosome 19p13 haplotype and the absence in 100 control chromosomes indicate that this I1811L variant is due to recurrent mutations rather than a common founder effect, while this finding renders its

Table 3. CACNL1A4 Mutations in Families with FHM or EA-2

Disease	Family	Location	Domain	Nucleotide Change		Consequence	
FHM	It-II	exon 4	I S4	nt 850	G→A	Arg_{192}→Gln (gain of SfcI site)	R192Q
FHM	US-P	exon 16	P-segment	nt 2272	C→T	Thr_{666}→Met	T666M
FHM	UK-B	exon 17	II S6	nt 2416	T→C	Val_{714}→Ala (gain of BbvI site)	V714A
FHM	NL-A/US-C	exon 36	IV S6	nt 5706	A→C	Ile_{1811}→Leu (gain of MnlI site)	I1811L
EA-2	CAN-191	exon 22	III S1	nt 4073	deletion C	frameshift (loss of NlaIV site)	$STOP_{1294}$
EA-2	CAN-26	intron 24	splice site	nt 4270+1	G→A	AC/gt→AC/at (loss of BsaAI site)	aberrant splicing

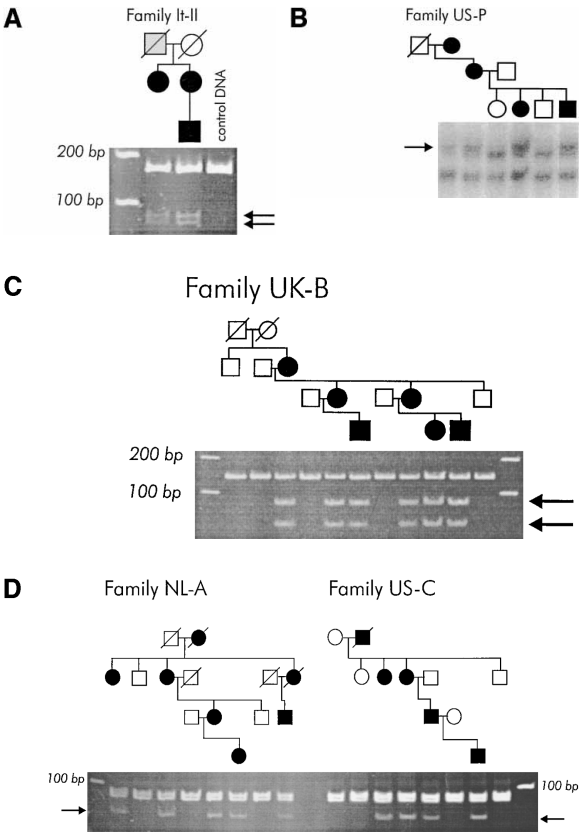

Figure 4. Mutation Detection in the CACNL1A4 Gene in FHM Families

Detection of four CACNL1A4 missense mutations in five different FHM families by restriction site (A, C, and D) or SSCP (B) analysis of PCR products. All missense mutations cosegregate with the disease within the families. Restriction site analysis: (A) exon 4 mutation (R192Q) in family *It-II* is recognized by SfcI digestion; control DNA consisted of DNA mixture of three unrelated individuals, (C) mutation V714A in family *UK-B* leads to additional BbvI site, and (D), mutation I1811L in families *NL-A* and *US-C* is detected by gain of MnlI restriction site. SSCP analysis: (B) aberrant SSCP conformers represent cosegregation of T666M mutation within family *US-P*. Arrows indicate positions of the aberrant bands in FHM affected individuals.

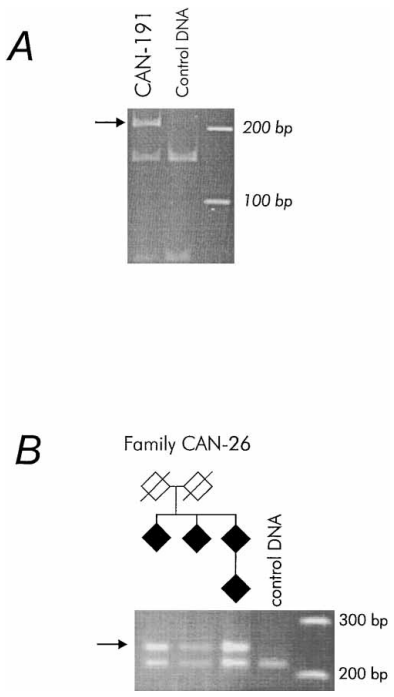

Figure 5. Mutation Detection in the CACNL1A4 Gene in EA-2 Families

Demonstration of EA-2 mutations by restriction site analysis of CACNL1A4 PCR products: (A) one basepair deletion (ΔC_{4073}) in *CAN-191* leads to loss of NlaIV restriction site in exon 22; (B) splice site mutation in intron 24 is shown by loss of BsaAI site in family *CAN-26*.

explanation as a rare polymorphism exceedingly unlikely. The V714A and I1811L missense mutations do not actually change the neutral-polar nature of the amino acid residues, but they are located at nearly the same position at the intracellular end of IIS6 and IVS6, while the original residues are conserved in all Ca^{2+} channel α1 subunit genes described (Stea et al., 1995).

Cerebellar atrophy in FHM families has been reported in ~40% of chromosome 19-linked FHM families but is not found in unlinked FHM families (Terwindt et al., 1996). We identified the same mutation (I1811L) in two different FHM families, of which only one also displays cerebellar atrophy in (some) affected family members. Apparently other factors than this amino acid substitution further contribute to the phenotypic variability. These factors may include genetic polymorphisms elsewhere in the gene or at other channel-related loci and the net effect of other ion channels on the polarity of the cell membrane.

Premature Stops in Episodic Ataxia Type-2

The identification of different mutations that are predicted to disrupt the reading frame of CACNL1A4 in two unrelated EA-2 patients provides strong evidence that CACNL1A4 is also involved in the pathogenesis of EA-2 (Table 3; Figure 5). In CAN-26, a basepair deletion (ΔC_{4073}) in codon 1266 leads to a frame-shift in the putative translation product and encounters a stop codon in the next exon (codon 1294). This frame-shift should yield a truncated Ca^{2+} channel α1 subunit consisting of repeat I and II, and a small portion of repeat III (IIIS1).

The G-to-A transition of the first nucleotide of intron 24 is affecting the highly conserved GT dinucleotide of the intronic 5′ splice junction. The brain-specific expression of CACNL1A4 precludes testing the hypothesis that this mutation produces aberrantly spliced RNAs by retaining the intron or utilizing other cryptic 5′ splice sites.

Molecular Mechanism of EA-2 and FHM

Identification of contrasting classes of mutations in EA-2 and FHM, premature stops and missense mutations, respectively, suggests different molecular mechanisms underlying the two disorders. The frame-shift and splice-site mutations in EA-2 are predicted to yield a truncated Ca^{2+} channel α1 subunit consisting of repeats I and II, and a part of repeat III (IIIS1). These peptides are unlikely to form functional Ca^{2+} channels and may either negatively influence P/Q Ca^{2+} channel assembly in the membrane (a dominant negative effect), or be unstable and

cause haploinsufficiency. A decrease of channel density according to either mechanism may lead to episodes of cerebellar dysfunction presenting as ataxia.

The four missense mutations identified in FHM suggest a different mechanism. It is likely that both alleles of the α1 subunit are expressed with the allele harboring a missense mutation resulting in gain-of-function variants of this Ca^{2+} channel α1 subunit. Such mutations have been described e.g. in the α subunit of the skeletal muscle sodium channel causing hyperkalemic periodic paralysis, paramyotonia congenita, and sodium channel myotonias (Hudson et al., 1995; Cannon, 1996). Each of these missense mutations codes for a substitution at highly conserved residues, leading to an impaired inactivation of the Na^{+}-channel. This example also demonstrates that different mutations in a single gene may result in marked phenotypic heterogeneity.

Implications for Migraine

Sib-pair analysis already showed significant involvement of the 19p13 FHM locus in migraine with and without aura (May et al., 1995). Therefore, the association of CACNL1A4 variants, notably the single missense variant (A454T) and the polymorphic trinucleotide (CAG) repeat in the 3′ noncoding region (Table 2), should now be investigated. The A454T variant, with an observed heterozygosity of 0.02, is located in the intracellular loop between IS6 and IIS1 (Figure 3). This region contains a conserved α interaction domain (AID) that binds β subunits (De Waard et al., 1996). The observed repeat length of $(CAG)_n$ varied from $n = 4$ to $n = 14$ and did not reach values of $n \geq 40$ typical for the highly unstable expanded trinucleotide repeats in, for example, individuals affected by spinocerebellar ataxia type-1 (Orr et al., 1993) or Huntington's disease (Huntington's Disease Collaborative Research Group, 1993). Still, such a trinucleotide repeat length may well affect, e.g., mRNA stability or the splicing efficiency and may interact with the transcript processing or translation. A minor change in mRNA stability may have a quantitative effect on the P/Q-type Ca^{2+} channels and may thus alter the threshold for internal or external trigger factors.

Identification of FHM and EA-2 as channelopathies opens new avenues for the development of prophylactic treatment. Most current models of migraine suggest that serotonin (5-hydroxytryptamine; 5-HT) plays a central role in migraine pathophysiology (Ferrari and Saxena, 1993). In migraine patients, 5-HT metabolism is disturbed: interictal systemic 5-HT levels are reduced and rise during attacks, possibly as a (failing) self-defense response (Ferrari et al., 1989). Effective specific acute anti-migraine drugs all share the ability to stimulate neuronal and vascular 5-HT1 receptors, thereby, among other effects, inhibiting release of vasoactive neuropeptides (Moskowitz, 1992; Ferrari and Saxena, 1995). Interestingly, P-type neuronal Ca^{2+} channels mediate 5-HT release (Codignola et al., 1993). Dysfunction of such channels, due to missense mutations, and thus inappropriate control of 5-HT release, may predispose patients for migraine attacks or may impair their self-aborting mechanism.

Because Mg^{2+} is known to interfere with Ca^{2+} channels (Altura, 1985; Zhang et al., 1992), our findings may also add to the growing evidence for involvement of magnesium in migraine pathophysiology. Magnetic resonance spectroscopy studies suggest that intracellular brain magnesium is reduced in migraineurs and that the regional distribution of brain magnesium is altered in patients with FHM (Ramadan et al., 1989). Furthermore, preliminary clinical trial data suggest that chronic administration of magnesium may reduce migraine attack frequency (Peikert et al., 1996).

Finally, Ca^{2+} and other ion channels are important in the mechanism of cortical spreading depression, which is believed to initiate migraine attacks (Lauritzen, 1996). Thus, impaired function of cerebral Ca^{2+} channels may facilitate the initiation of attacks.

Even though we have demonstrated a role for this chromosome 19p13 locus in $\sim$50% of FHM families (Ophoff et al., 1994) and a contribution to common forms of migraine (May et al., 1995), it is evident that additional genes need to be identified to explain the full spectrum of FHM and migraine. The functional P/Q-type Ca^{2+} channel is a multisubunit complex consisting of β, α2, and δ subunits in addition to the α1 subunit described here. Genes for those subunits and other interacting proteins should be considered as potential candidate genes for non-chromosome 19-linked FHM and for migraine with or without aura.

In conclusion, our findings implicate the brain-specific P/Q-type Ca^{2+} channel α1-subunit gene on chromosome 19p13.1 (CACNL1A4) in the pathogenesis of both EA-2 and FHM, and most likely also of the more common forms of migraine. Insight into the structure and function of this gene will improve diagnosis and may provide a rationale for the development of specific prophylactic therapy for migraine and other paroxysmal cerebral disorders.

Experimental Procedures

Subjects

Sixteen FHM patients were selected, including eight individuals from four unrelated chromosome 19-linked FHM families (*NL-A*, *UK-B*, *US-C* [Ophoff et al., 1994], and *US-P* [Elliot et al., 1996]), two affected individuals from two small FHM families from Italy (*It-I* and *-II*), and six individuals with sporadic hemiplegic migraine (i.e., no other family member was shown to suffer from attacks of hemiplegic migraine). In families *NL-A* and *US-P* cerebellar ataxia and/or nystagmus is associated with FHM. An additional set of four subjects from four unrelated EA-2 families linked to chromosome 19 was also included (*CAN-25*, *-45*, *-191*, *-197*). Fifty randomly collected individuals from the Dutch population were used as a control to determine the allele frequencies of polymorphic sites.

Exon Trap Experiments

Exon trapping was performed according to Buckler et al. (1991). In brief, eight cosmids from the candidate region (LLNL no. 31563, 23883, 26540, 17498, 31583, 14268, 26432, 20618) were completely digested with BamHI, BglII, and BamHI/BglII. The pooled fragments were randomly cloned into the BamHI site of the pSPL3 vector. Plasmid DNA was used to transfect COS1 cells. Total RNA was isolated from the COS1 cells 48 hr after transfection, cDNA was synthesized, and PCR products (amplified using vector-specific primers) were subcloned (TA cloning kit, Invitrogen) and sequenced.

cDNA Sequence

Two fragments of cDNA sequences (based on exon trapping and BLAST search, respectively) were amplified and used as probes for

screening a human cerebellum cDNA library (Clontech). Amplimers for PCR of the first probe (600 bp; containing trapped exons) were forward 5′-TAGCGAATTGCATCATCCTCGC-3′ and reversed 5′-CCACCCTTCCATGGTTATGC-3′. The second probe (480 bp) was amplified by forward primer 5′-TGCGAGAGATGGGCAGAGAT-3′ and reversed primer 5′-TGGGCATAGCGGTCCTTGTC-3′. Rather than going through multiple rounds of hybridizations, the correct inserts of positive plaques were amplified after a primary screening, using a combination of cDNA- and vector-specific oligonucleotide primers. Simultaneously, primers were designed based on sequences identical in rabbit (EMBL X57476) and rat (GenBank M64373) cDNA. These primers were succesfully used for a direct amplification of fragments of cDNA from total human cerebellum cDNA; PCR products were cloned (TA cloning kit, InVitroGen) and sequenced.

Northern Blot Analysis

Northern blot was prepared containing total RNA (20 μg/lane) of several tissues from rhesus monkey (total brain, cerebellum, cortex, hypothalamus, muscle, heart, kidney, liver) as well as total RNA from human lymphocytes and mouse skin tissue. Total RNA was isolated as previously described (Chomczynski and Sacchi, 1987). Hybridization was performed in Church buffer for 16 hr at 65°C using α-^{32}P-labeled cDNA probe 1 (section cDNA sequence). The blot was washed at 65°C and to a stringency of 0.3× SSC/0.1% SDS.

Genomic Structure

Ten different cosmids from the contig extending the CACNL1A4 gene (Figure 1) were subcloned separately in either M13 or pBlue-Script KS (Stratagene) vector. From each cosmid library, at least 3 × 96 random clones with an average insert size of about 2 kb were picked. Positive clones were identified by hybridization techniques and subsequently sequenced with vector-specific primers; intron-exon boundary sequences were completed using cDNA-based primers.

Mutation Analysis, DHPLC and SSCP

Genomic DNA was used as template to generate polymerase chain reaction (PCR) products for single-strand conformational polymorphism (SSCP) analysis and denaturing high-performance liquid chromatography (DHPLC), a heteroduplex-based screening (Oefner and Underhill, 1995; Hayward-Lester et al., 1996). Amplifications were performed according to standard procedures, using the primer pairs listed in Table 1. Except for the 5′ side of exon 6, primers were chosen to produce fragments that contained a single exon and at least 35 basepairs (including primer) of each flanking intron sequence. Amplification of exons 1 and 20 was performed producing two overlapping fragments and exon 19 was amplified into three overlapping fragments.

DHPLC was carried out on automated HPLC instrumentation. Crude PCR products, which had been subjected to an additional 3 min 95°C denaturing step followed by gradual reannealing from 95°C to 65°C over a period of 30 min prior to analysis, were eluted with a linear acetonitrile (9017–03, J. T. Baker, Phillipsburg, NJ, USA) gradient of 1.8%/min at a flow-rate of 0.9 ml/min. The start- and end-points of the gradient were adjusted according to the size of the PCR products (Huber et al., 1995). The temperature required for successful resolution of heteroduplex molecules was determined empirically by injecting one PCR product of each exon at increasing mobile phase temperatures until a significant decrease in retention was observed (Figure 6).

For SSCP analysis, primary PCR products were labeled by incorporation of [α-^{32}P]dCTP in a second round of PCR. Samples were diluted and denatured in formamide buffer before electrophoresis. SSCP was carried out according to published protocols (Orita et al., 1989; Ravnik-Glavac et al., 1994).

Sequencing of PCR products was performed with an ABI 377 automated sequencing apparatus with cycle sequencing according to the manufacturer. Furthermore, PCR products were cloned in the TA vector (Invitrogen) and subjected to manual dideoxy sequence analysis (T7 Sequencing kit, Pharmacia Biotech).

Subsequent to sequence analysis, the presence of a mutation was confirmed by gain or loss of restriction sites. Eight μl of crude PCR product of at least one affected individual and one unaffected control was digested with 3 U of appropriate restriction enzyme (Table 3) in 20 μl reaction volume for 6 hr at 37°C, according to the manufacturer's instructions.

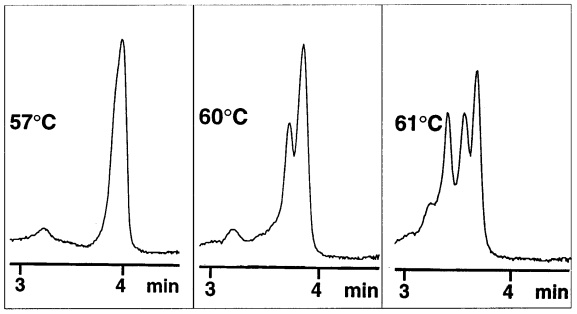

Figure 6. Mutation Screening by Denaturing High Performance Liquid Chromatography (DHPLC)

Chromatograms of DHPLC analysis of heterozygote PCR product at increasing mobile phase temperatures (57°C–61°C). Successful resolution of heteroduplex signal of exon 32 of family member of *NL-A* was accomplished at 61°C.

Acknowledgments

The authors wish to thank Steve Peroutka (Menlo Park) for providing DNA samples of family US-P. Angelika Hahn and Donald Lewis (London, Ontario) and Paola Carrera and Laura Vismara (Milan) are acknowledged for their contribution in characterization of the EA-2 families, and the Italian FHM families, respectively. Michel van Geel and Richard Lemmers are acknowlegded for their technical assistance in exon trapping and RNA isolations. We also thank Riccardo Fodde, Lodewijk Sandkuijl, and Cisca Wijmenga for their valuable discussions and critical comments on the manuscript. This work has been supported by the Phoenix Foundation (R. A. O.) and The Netherlands Organization for Scientific Research (NWO) (number 950-10-615; G. M. T.). D. E. B. is a Scholar of the MRC and his work is funded by the MRC. The work of M. F. is funded by Theleton-Italy, no. 179. Work performed by the Lawrence Livermore National Laboratory (LLNL) under auspices of the U.S. Department of Energy, under contract no. W-7405-Eng-48.

Received August 28, 1996.

References

Altura, B.M. (1985). Calcium antogonist properties of magnesium: implications for antimigraine actions. Magnesium *4*, 169–175.

Browne, D.L., Gancher S.T., Nutt, J.G., Brunt, E.R., Smith, E.A., Kramer, P., and Litt, M. (1994). Episodic ataxia/myokymia syndrome is associated with point mutations in the human potassium channel gene, KCNA1. Nat. Genet. *8*, 136–140.

Buckler, A.J., Chang, D.D., Graw, S.L., Brook, J.D., Haber, D.A., Sharp, P.A., and Housman, D.E. (1991). Exon amplification: a strategy to isolate mammalian genes based on RNA splicing. Proc. Natl. Acad. Sci. USA *88*, 4005–4009.

Campbell, K.P., Leung, A.T., and Sharp, A.H. (1988). The biochemistry and molecular biology of the dihydropyridine-sensitive calcium channel. Trends Neurosci. *11*, 425–430.

Cannon, S.C. (1996) Ion-channel defects and aberrant excitability in myotonia and periodic paralysis. Trends Neurosci. *19*, 3–10.

Chomczynski, P., and Sacchi, N. (1987). Single step method of RNA isolation by acid guanidium thiocyanate phenol chloroform extraction. Anal. Biochem. *162*, 156–159.

Codignola, A., Tarroni, P., Clementi, F., Pollo, A., Lovallo, M., Carbone, E., and Sher, E. (1993). Calcium channel subtypes controlling serotonin release from human small cell lung carcinoma cell lines. J. Biol. Chem. *268*, 26240–26247.

De Waard, M., Gurnett, C.A., and Campbell, K.P. (1996). Structural and functional diversity of voltage-activated calcium channels. In Ion Channels, Volume 4, T. Narahashi, ed. (New York: Plenum Press).

Diriong, S., Lory, P., Williams, M.E., Ellis, S.B., Harpold, M.M., and Taviaux, S. (1995). Chromosomal localization of the human genes for α1A, α1B, and α1E voltage-dependent Ca^{2+} channel subunits. Genomics *30*, 605–609.

Elliott, M.A., Peroutka, S.J., Welch, S., and May, E.F. (1996). Familial Hemiplegic Migraine, nystagmus, and cerebellar atrophy. Ann. Neurol. *39*, 100–106.

Ferrari, M.D., and Saxena, P.R. (1993). On serotonin and migraine: a clinical and pharmacological review. Cephalalgia. *13*, 151–165.

Ferrari, M.D., and Saxena, P.R. (1995). 5-HT1 receptors in migraine pathophysiology and treatment. Eur. J. Neurol. *2*, 5–21.

Ferrari, M.D., Odink, J., Tapparelli, C., Van Kempen, G.M., Pennings, E.J., and Bruyn, G.W. (1989). Serotonin metabolism in migraine. Neurology *39*, 1239–1242.

Griggs, R.C., and Nutt, J.G. (1995). Episodic ataxias as channelopathies. Ann. Neur. *37*, 285–286.

Guy, H.R., and Durell, S.R. (1996). Three-dimensional models of ion channel proteins. In Ion Channels, Volume 4, T. Narahashi, ed. (New York, Plenum Press).

Haan, J., Terwindt, G.M., and Ferrari, M.D. (1996). Genetics of migraine. In Advances in Headache, N.T. Mathew, ed. (Philadelphia, PA: W.B. Saunders), in press.

Hayward-Lester, A., Chilton, B.S., Underhill, P.A., Oefner, P.J., and Doris, P.A. (1996) Quantification of specific nucleic acids, regulated RNA processing and genomic polymorphisms using reversed-phase HPLC. In Gene Quantification, F. Ferr, ed. (Basel, Switzerland: Birkhuser Verlag).

Headache Classification Committee of the International Headache Society (1988). Classification and diagnostic criteria for headache disorders, cranial neuralgias and facial pain. Cephalalgia *8*, 19–28.

Huber, C.G., Oefner, P.J., and Bonn, G.K. (1995) Rapid and accurate sizing of DNA fragments by ion-pair chromatography on alkylated nonporous poly(styrene-divinylbenzene) particles. Anal. Chem. *67*, 578–585.

Huntington's Disease Collaborative Research Group (1993). A novel gene containing a trinucleotide repeat that is expanded and unstable on Huntington's disease chromosomes. Cell *72*, 971–983.

Hudson, A.J., Ebers, G.C., and Bulman, D.E. (1995). The skeletal muscle sodium and chloride channel diseases. Brain *118*, 547–563.

Joutel, A., Bousser, M-G., Biousse, V., Labauge, P., Chabriat, H., Nibbio, A., Maciazek, J., Meyer, B., Bach, M.A., Weissenbach, J., et al. (1993). A gene for familial hemiplegic migraine maps to chromosome 19. Nature Genet. *5*, 40–45.

Joutel, A., Ducros, A., Vahedi, K., Labauge, P., Delrieu, O., Pinsard, N., Mancini, J., Ponsot, G., Gouttiere, F., Gastaut, J.L., et al. (1994). Genetic heterogeneity of familial hemiplegic migraine. Am. J. Hum. Genet. *55*, 1166–1172.

Jurkatt-Rott, K., Lehman-Horn, F., Elbaz, A., Heine, R., Gregg, R.G., Hogan, K., Powers, P.A., Lapie, P., Val-Santos, J.E., Weissenbach, J., et al. (1994). A calcium channel mutation causing hypokalemic periodic paralysis. Hum. Mol. Genet. *3*, 1415–1419.

Kramer, P.L., Yue, Q., Gancher, S.T., Nutt, J.G., Baloh, R., Smith, E., Browne, D., Bussey, K., Lovrien, K., Nelson, S., and Litt, M. (1995). A locus for the nystagmus-associated form of episodic ataxia maps to an 11-cM region on chromosome 19p. Am. J. Hum. Genet. *57*, 182–185.

Lauritzen, M. (1996). Pathophysiology of the migraine aura. Sci. Med. *3*, 32–41.

Margolis, R.L., Breschel, T.S., Li, S.H., Kidwai, A.S., Antonarakis, S.E., McInnis, M.G., Ross, C.A. (1995). Characterization of cDNA clones containing CCA trinucleotide repeats derived from human brain. Som. Cell Mol. Genet. *21*, 279–284.

May, A., Ophoff, R.A., Terwindt, G.M., Urban, C., Van Eijk, R., Haan, J., Diener, H.C., Lindhout, D., Frants, R.R., Sandkuijl, L.A., and Ferrari, M.D. (1995). Familial hemiplegic migraine locus on 19p13 is involved in the common forms of migraine with and without aura. Hum. Genet. *96*, 604–608.

Mori, Y., Friedrich, T., Kim. M.S., Mikami, A., Nakai., J., Ruth, P., Bosse, E., Hofmann, F., Flockerzi, V., Furuichi, T., et al. (1991). Primary structure and functional expression from complementary DNA of a brain calcium channel. Nature *350*, 398–402.

Moskowitz, M.A. (1992). Neurogenic versus vascular mechanism of sumatriptan and ergot alkaloids in migraine. Trends Pharmacol. Sci. *13*, 307–311.

Oefner, P.J., and Underhill, P.A. (1995). Comparative DNA sequencing by denaturing high-performance liquid chromatography (DHPLC). Am. J. Hum. Genet. *57* [Suppl.], A266.

Ophoff, R.A., Van Eijk R., Sandkuijl, L.A., Terwindt, G.M., Grubben, C.P.M., Haan, J., Lindhout, D., Ferrari, M.D., and Frants, R.R. (1994). Genetic heterogeneity of familial hemiplegic migraine. Genomics *22*, 21–26.

Ophoff, R.A., Terwindt, G.M., Vergouwe, M.N., Van Eijk, R., Mohrenweiser, H., Litt, M., Hofker, M.H., Ferrari, M.D., and Frants, R.R. (1996). A 3 Mb region for the Familial Hemiplegic Migraine locus on 19p13.1-p13.2; exclusion of PRKCSH as a candidate gene. Eur. J. Hum. Genet., in press.

Orita, M., Suzuki, Y., Sekiya, T., and Hayashi, K. (1989). Rapid and sensitive detection of point mutations and DNA polymorphisms using the polymerase chain reaction. Genomics *5*, 874–879.

Orr, H.T., Chung, M.Y., Banfi, S., Kwiatkowski, T.J., Servadio, A., Beaudet, A.L., McCall, A.E., Duvick, L.A., Ranum, L.P., and Zoghbi, H.Y. (1993). Expansion of an unstable trinucleotide CAG repeat in spinocerebellar ataxia type 1. Nature Genet. *4*, 221–226.

Peikert, A., Wilimzig, C., and Köhne-Volland, R. (1996). Prophylaxis of migraine with oral magnesium: results from a prospective, multicenter, placebo-controlled and double-blind randomized study. Cephalalgia *16*, 257–263.

Ptacek, L.J., George, A.L., Griggs, R.C., Tawil, R., Kallen, R.G., Barchi, R.L., Robertson, M., and Leppert, M.F. (1991). Identification of a mutation in the gene causing hyperkalemic periodic paralysis. Cell *67*, 1021–1027.

Ptacek, L.J., Tawil, R., Griggs, R.C., Engel, A.G., Layzer, R.B., Kwiecinski, H., McManis, P.G., Santiago, L., Moore, M., Fouad, G., et al. (1994). Dihydropyridine receptor mutations cause hypokalemic periodic paralysis. Cell *77*, 863–868.

Ramadan, N.M., Halvorson, H., Vande-Linde, A., Levine, S.R., Helpern, J.A., and Welch, K.M.A. (1989). Low brain magnesium in migraine. Headache *29*, 416–419.

Ravnik-Glavac, M., Glavac, D., and Dean, M. (1994). Sensitivity of single-strand conformation polymorphism and heteroduplex method for mutation detection in the cystic fibrosis gene. Hum. Mol. Genet. *3*, 801–807.

Russell, M.B., and Olesen, J. (1995). Increased familial risk and evidence of genetic factor in migraine. Br. Med. J. *311*, 541–544.

Russell, M.B., Rasmussen B K., Thorvaldsen P., and Olesen J. (1995). Prevalence and sex-ratio of the subtypes of migraine. Int. J. Epidemiol. *24*, 612–618.

Starr, T.V.B., Prystay, W., and Snutch, T. (1991). Primary structure of a calcium channel that is highly expressed in the rat cerebellum. Proc. Natl. Acad. Sci. USA *88*, 5621–5625.

Stea, A., Soong, T.W., and Snutch, T.P. (1995). Voltage-gated calcium channels. In Ligand- and Voltage-Gated Ion Channels, R.A. North, ed. (CRC Press), pp. 113–151.

Tanabe, T., Takeshima, H., Mikami, A., Flockerzi, V., Takahashi, H., Kangawa, K., Kojima, M., Matsuo, H., Hirose, T., and Numa, S. (1987). Primary structure of the receptor for calcium channel blockers from skeletal muscle. Nature *328*, 313–318.

Teh, B.T., Silburn, P., Lindblad, K., Betz, R., Boyle, R., Schalling, M., and Larsson, C. (1995). Familial periodic cerebellar ataxia without myokymia maps to a 19-cM region on 19p13. Am. J. Hum. Genet. *56*, 1443–1449.

Terwindt, G.M., Ophoff, R.A., Haan, J., Frants, R.R., and Ferrari, M.D. (1996). Familial hemiplegic migraine: a clinical comparison of

families linked and unlinked to chromosome 19. Cephalagia *16*, 153–155.

Von Brederlow, B., Hahn, A.F., Koopman, W.J., Ebers, G.C., and Bulman, D. (1995). Mapping the gene for acetozolamide responsive hereditary paroxysmal cerebellar ataxia to chromosome 19p. Hum. Mol. Genet. *2*, 279–284

Zhang, A., Cheng, T.P.O., and Altura, B.M. (1992). Magnesium regulates intracellular free ionized calcium concentration and cell geometry in vascular smooth muscle cell. Biochem. Biophys. Acta *1134*, 25–29.